JACS
JOURNAL OF THE AMERICAN CHEMICAL SOCIETY

Communication

pubs.acs.org/JACS

A General Strategy for the Semisynthesis of Ratiometric Fluorescent Sensor Proteins with Increased Dynamic Range

Lin Xue, Efthymia Prifti, and Kai Johnsson*

Institute of Chemical Sciences and Engineering (ISIC), Institute of Bioengineering, National Centre of Competence in Research (NCCR) Chemical Biology, École Polytechnique Fédérale de Lausanne (EPFL), 1015 Lausanne, Switzerland

Supporting Information

ABSTRACT: We demonstrate how a combination of self-labeling protein tags and unnatural amino acid technology permits the semisynthesis of ratiometric fluorescent sensor proteins with unprecedented dynamic range *in vitro* and on live cells. To generate such a sensor, a binding protein is labeled with a fluorescent competitor of the analyte using SNAP-tag in conjugation with a second fluorophore that is positioned in vicinity of the binding site of the binding protein using unnatural amino acid technology. Binding of the analyte by the sensor displaces the tethered fluorescent competitor from the binding protein and disrupts fluorescence resonance energy transfer between the two fluorophores. Using this design principle, we generate a ratiometric fluorescent sensor protein for methotrexate that exhibits large dynamic ranges both *in vitro* (ratio changes up to 32) and on cell surfaces (ratio change of 13). The performance of these semisynthetic sensor proteins makes them attractive for applications in basic research and diagnostics.

Ratiometric fluorescent sensors are powerful tools for noninvasive quantification of analytes with high spatio-temporal resolution in living cells and complex biological samples.[1,2] Such sensors are generally based on a binding protein for an analyte of interest that is expressed as fusion protein with two fluorescent proteins capable of fluorescence resonance energy transfer (FRET). Binding of the analyte induces a conformational change in the binding protein that results in a change in the FRET efficiency between the two fluorescent proteins. However, such sensors often suffer from limited dynamic range, with maximal emission ratio changes (ΔR_{max}) <10-fold.[2,3] The rather low dynamic range often restricts their utility. Furthermore, the underlying design principle requires the identification of a binding protein that undergoes a conformational change upon analyte binding, which is not trivial for numerous analytes. We have previously introduced FRET-based semisynthetic biosensors, so-called **SN**AP-tag based **i**ndicator with a **f**luorescent **i**ntramolecular **t**ether (Snifits), which do not rely on conformational changes of binding proteins (Figure 1a).[4] Snifits are comprised of SNAP-tag,[5] a fluorescent protein (for example CLIP-tag[6] labeled with an appropriate fluorophore), and a binding protein for the analyte of interest. SNAP-tag is labeled with a molecule composed of a ligand for the binding protein and a fluorophore suitable for FRET. In the absence of free analyte, the tethered ligand binds to the binding protein, resulting in high FRET between the two fluorophores. In the presence of analyte, the tethered ligand is displaced from the binding protein, thereby reducing the FRET efficiency. The approach is compatible with various receptor proteins, and Snifits for glutamate, GABA, acetylcholine, and several synthetic drugs have been generated.[7] However, Snifits also suffer from modest ratio changes (ΔR_{max} up to 5) as the large size of the two proteins carrying the fluorophores prevents close proximity of the latter in the closed state of the sensor. Here we introduce a general solution to this issue by positioning a fluorophore near the binding site of the binding protein using unnatural amino acid technology (Figure 1b),[8] creating so-called **u**Snifits with unprecedented FRET ratio changes both *in vitro* and on the surface of live cells.

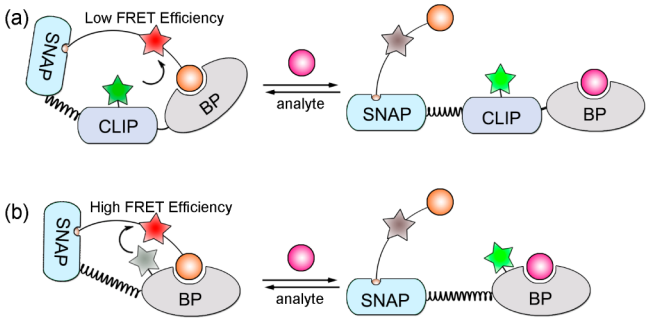

Figure 1. Increasing the dynamic range of Snifits through incorporation of unnatural amino acids. (a) A traditional Snifit is a fusion protein of SNAP-tag, CLIP-tag, and a binding protein (BP). SNAP-tag is labeled with a molecule containing a fluorophore (red star) and a ligand (orange ball) that binds to BP; CLIP-tag is labeled with a second fluorophore (green star). (b) In uSnifit, CLIP-tag is replaced by a fluorophore-labeled unnatural amino acid near the binding site of BP, which should increase FRET efficiency in absence of analyte.

To demonstrate the feasibility of the approach, we decided to generate uSnifits for the important anticancer and anti-inflammatory drug methotrexate (MTX). *E. coli* dihydrofolate reductase (eDHFR) was selected as binding protein, as eDHFR has been successfully used in the past for the generation of bioluminescent sensor proteins and various ligands suitable for intramolecular binding have been described.[9] As an intramolecular ligand we chose the eDHFR inhibitor trimethoprim (TMP) connected to benzylguanine, the substrate of SNAP-tag via a linker containing Cy5 as fluorophore (Figure 2a,b). We

Received: March 23, 2016
Published: April 12, 2016

DOI: 10.1021/jacs.6b03034
J. Am. Chem. Soc. 2016, 138, 5258−5261

prepared derivatives with three different linker lengths between TMP ligand and Cy5 to investigate the effect of linker lengths on FRET efficiency.

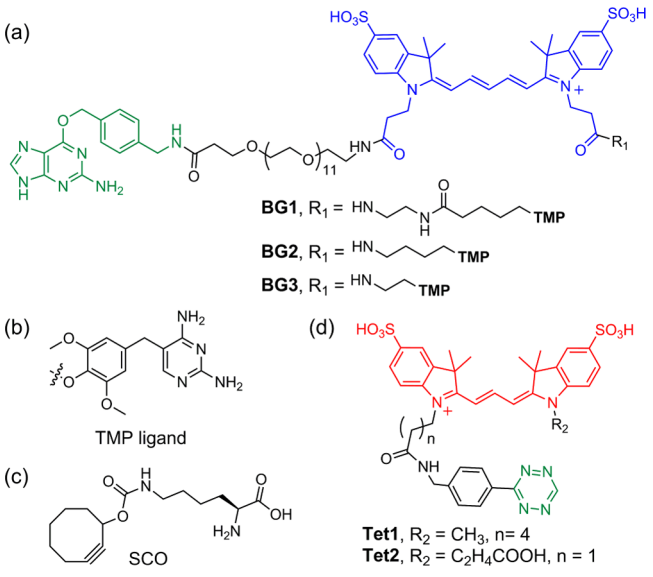

Figure 2. Molecules used for MTX-uSnifits. (a) Probes for labeling of SNAP-tag containing the SNAP-tag substrate benzylguanine (BG) (green) and the fluorophore sulfo-Cy5 (blue) connected to TMP ligand via different linkers. (b) Structure of TMP-like ligand. (c) Structure of SCO. (d) Probes for labeling of the unnatural amino acid contain a tetrazine (green) moiety and a fluorophore sulfo-Cy3 (red).

Inspection of the crystal structure of eDHFR with MTX suggested N23, L36, and G51 as residues for fluorophore labeling via an unnatural amino acid, as these residues are in the direct vicinity of the bound ligand but should be tolerant to mutagenesis (Figure 3). For the incorporation of unnatural

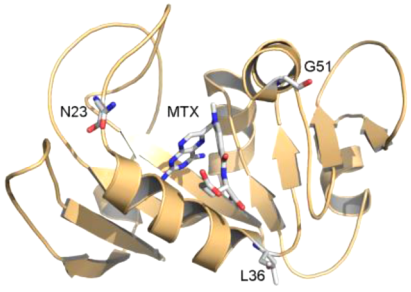

Figure 3. Crystal structure of eDHFR (PDB entry: 2INQ). The N23, L36, and G51 residues for incorporation of an unnatural amino acid and the bound MTX are highlighted.

amino acids we chose an engineered pyrrolysine tRNA synthetase/tRNA pair from *Methanosarcina* species as this system has been shown to be well-suited for incorporation of diverse unnatural amino acids in desired proteins.[10] As unnatural amino acid we chose cyclooctyne lysine (SCO, Figure 2c), which can be specifically labeled with tetrazine derivatives via strain-promoted inverse electron demand Diels–Alder cycloaddition.[11] We prepared two different tetrazines in which the linker between the fluorophore and the tetrazine varied (Figure 2d). The protein component of MTX-uSnifit is comprised of an eDHFR mutant fused to SNAP-tag via polyproline (P30) linker (SNAP_-P30_eDHFR). The rigid proline linker serves to increase the distance between the two fluorophores in the open state of the sensor. To increase the rate with which the sensor responds to changes in analyte concentration, we decreased the affinity of eDHFR for NADPH by introducing the mutations R44L and H45Q,[12] as we found that cooperative binding of NADPH and tethered ligand to eDHFR reduced the off-rate of bound ligand. For benchmarking, we also generated a traditional MTX-Snifit (SNAP_P30_CLIP_eDHFR) in which Cy3 was attached via CLIP-tag instead of an unnatural amino acid (Figure 1a).

The three MTX-uSnifits with SCO incorporated at N23, L36, or G51 were expressed and purified in *E. coli* DH10B cells (Table S1 and Figure S1). After labeling with the BG and tetrazine derivatives (Figure 2), the fluorescence emission spectra of the resulting 18 sensors were measured as a function of the MTX concentration (Figure 4 and Table 1). For all of the MTX-Snifits,

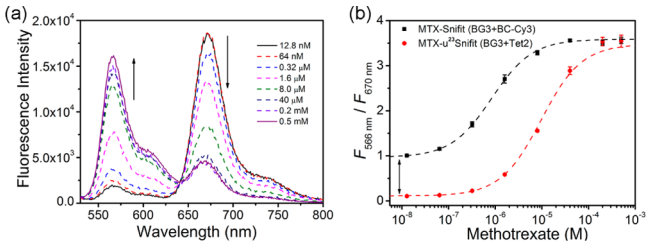

Figure 4. (a) Emission spectra of MTX-u^{23}Snifit (BG3 + Tet2) upon the titration of MTX (12.8 nM to 0.5 mM) in HEPES buffer as a representative example for the MTX-uSnifits. (b) Fluorescence intensity ratio ($F_{566}/F_{670\ nm}$) responses of MTX-u^{23}Snifit (BG3 + Tet2) and MTX-Snifit (BG3 + BC-Cy3) as a function of MTX concentration. The data (mean ± SD) are fitted to a single-site binding isotherm (dashed line).

titration with increasing concentrations of MTX led to a decrease of the fluorescence emission of Cy5 and an increase of Cy3 fluorescence, which is in line with MTX displacing the tethered TMP ligand. For each of the 18 sensors, the maximal emission ratio change (ΔR_{max}) was above 10 and reached 30 for those MTX-uSnifits with short linkers between the fluorophores and both TMP and tetrazine, respectively (Table 1). The increase in ΔR_{max} through shortening of the linkers can be rationalized by considering that this should reduce the distance between the two fluorophores in the closed state of the uSnifits. To confirm that the observed ratio changes were due to changes in FRET efficiency but not an environmental effect on the fluorescence properties of the tethered Cy5, we investigated the effect of opening and closing of the sensors on the tethered Cy5. We labeled MTX-u^{23}Snifit with BG1, BG2, or BG3 only and measured the Cy5 fluorescence intensity in the presence and absence of high concentrations of MTX (Figure S2). The environmental effects on tethered Cy5 were modest; the largest effect was seen when the sensor was labeled with BG3, which showed a ~ 26% decrease in fluorescence intensity upon sensor opening. These results confirm that the observed maximal ratio changes are mainly due to changes in FRET efficiency. The fact that uSnifits with large dynamic ranges were obtained for all three sites chosen for the incorporation of the unnatural amino acid underlines the generality of the approach. The observed maximal emission ratio changes of our MTX-uSnifits are, to the best of our knowledge, the highest changes for any FRET-based ratiometric fluorescent sensor protein reported so far. It is instructive to compare the performance of the uSnifits with a traditional MTX-Snifit in which Cy3 is attached via CLIP-tag (see Figure 1a).

DOI: 10.1021/jacs.6b03034
J. Am. Chem. Soc. 2016, 138, 5258–5261

Table 1. ΔR_{max}, C_{50}, and K_d^{comp} of the MTX-Snifit and MTX-uSnifits with different label pairs.[a]

	BG1			BG2			BG3		
protein (+ Cy3 label)	ΔR_{max}	C_{50} (μM)	K_d^{comp} (μM)	ΔR_{max}	C_{50} (μM)	K_d^{comp} (μM)	ΔR_{max}	C_{50} (μM)	K_d^{comp} (μM)
MTX-Snifit (+ BC-Cy3)	2.5	0.25 ± 0.03	0.12 ± 0.01	2.7	0.23 ± 0.08	0.11 ± 0.01	3.7	0.84 ± 0.06	0.29 ± 0.03
MTX-u^{23}Snifit (+ Tet1)	11.1	3.26 ± 0.06	1.07 ± 0.03	12.7	4.20 ± 0.92	1.28 ± 0.02	18.4	8.30 ± 0.43	2.48 ± 0.05
MTX-u^{23}Snifit (+ Tet2)	21.4	3.32 ± 0.13	0.93 ± 0.01	22.6	4.13 ± 0.25	1.18 ± 0.06	31.8	9.62 ± 0.89	2.36 ± 0.10
MTX-u^{36}Snifit (+ Tet1)	13.4	3.49 ± 0.17	1.20 ± 0.05	15.1	3.06 ± 0.13	1.05 ± 0.04	25.7	7.32 ± 0.40	1.95 ± 0.07
MTX-u^{36}Snifit (+ Tet2)	14.3	2.92 ± 0.09	0.86 ± 0.09	19.1	2.32 ± 0.09	0.83 ± 0.03	29.8	5.48 ± 0.31	1.42 ± 0.06
MTX-u^{51}Snifit (+ Tet1)	17.4	4.70 ± 0.07	1.50 ± 0.03	18.9	5.13 ± 0.13	1.81 ± 0.08	24.4	10.52 ± 0.36	2.89 ± 0.11
MTX-u^{51}Snifit (+ Tet2)	23.0	3.31 ± 0.15	0.97 ± 0.03	25.6	3.25 ± 0.12	1.09 ± 0.04	34.2	7.57 ± 0.28	2.02 ± 0.05

[a] C_{50} and K_d^{comp} are defined as the analyte concentration that resulted in half-maximum ratio change and half-opening of the sensor, respectively.

ΔR_{max} for MTX-Snifit was measured to be 3.7 (Table 1 and Figure 4b), thus almost a factor of 10 below that of the corresponding uSnifits. Using FRET as a molecular ruler, we also calculated the distances between the two fluorophores in the closed state of the sensors for the traditional MTX-Snifit and the MTX-u^{23}Snifit (Table S2).[13] Whereas for MTX-Snifit (BG3 + BC-Cy3) the apparent distance between the two fluorophores in the closed state of the sensor was estimated to be 56.0 Å, the apparent distance between the two fluorophores in MTX-u^{23}Snifit (BG3 + Tet2) was measured to be 38.5 Å. In contrast, the distances between the fluorophores in their open state were measured to be around 60 Å for both sensors. These data further underline to what degree the use of unnatural amino acids allows optimizing sensor design.

Another characteristic of the sensor is the dissociation constant, K_d^{comp}, which is the concentration of the analyte at which the sensor is half-open (see SI for calculations). The K_d^{comp} values for MTX-uSnifits varied around 1−3 μM and are about 10-fold higher than those measured for the corresponding traditional MTX-Snifit. This might be rationalized by the fact that the unnatural amino acid was incorporated in the direct vicinity of the active site, potentially resulting in unfavorable interactions with the bound ligand. Furthermore, we evaluated the selectivity of MTX-u^{23}Snifit for relevant key metabolites of MTX, 7-OH MTX, and 4-deoxy-4-amino-*N*-methylpteroic acid. As shown in Figure S4, both metabolites did not interact with the sensor at physiological relevant concentrations, which is a prerequisite for using our MTX-uSnifit for quantification of MTX in biological (clinical) samples.

Labeling through unnatural amino acid technology and SNAP-tag has been shown to be highly specific and can even be carried out *in vivo*,[14] thereby opening up the possibility for semisynthesis of uSnifits in live cells. In such an application the protein component would be expressed in the cell of interest and subsequently rendered functional through chemical labeling. To test the feasibility of the approach, we attempted to express MTX-uSnifit on the surface of mammalian cells. Specifically, we expressed MTX-u^{23}Snifit on the surface of HEK293T cells via a C-terminal PDGFR transmembrane domain, which displayed the sensor on the extracellular surface. After labeling HEK293T cells with 2 μM BG3 and 10 μM tetrazine derivatives, we observed an colocalization of Cy3 and Cy5 fluorescence at the plasma membrane, indicating specific dual labeling (Figures 5a–c and S5).

Perfusion of MTX over the cells expressing labeled MTX-u^{23}Snifit (BG3 + Tet2) resulted in a sharp fluorescence intensity increase in the Cy3 channel and a concomitant decrease in the Cy5 channel (Figure S6). In these experiments we observed a ΔR_{max} = 12.5, which can be fully reversed by washing out MTX (Figure S6). The observed ΔR_{max} on live cells is significantly

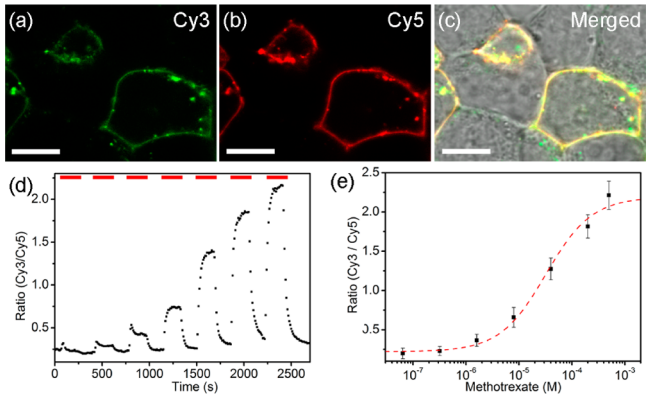

Figure 5. MTX-u^{23}Snifit was expressed on the surface of HEK293T cells and was labeled with Tet2 and BG3. (a) Cy3 channel. (b) Cy5 channel. (c) Overlay of Cy3 channel, Cy5 channel, and transmission channel. Scale bar is 10 μm. (d) Time course of perfusion of MTX-u^{23}Snifit (BG3 + Tet2) with increasing concentrations of MTX. The red bar indicates the time span of perfusion with MTX. Concentrations from left to right: 64 nM, 0.32 μM, 1.6 μM, 8 μM, 40 μM, 0.2 mM, 0.5 mM. (e) Fitting the MTX titration curve of MTX-u^{23}Snifit (BG3 + Tet2) on the extracellular surface of HEK293T cells with a single-site binding isotherm (dashed line).

smaller than that measured *in vitro* ($\Delta R_{max}^{in\ vitro}$ = 31.8). A similar trend was also observed for MTX-u^{23}Snifit labeled with BG3 and Tet1, which showed ΔR_{max} = 18.4 *in vitro* but ΔR_{max} = 7.1 on the surface of HEK293T cells (Figure S7). We believe that the differences in ΔR_{max} values *in vitro* and in live-cell imaging experiments resulted from the non-negligible fluorescence background in the live-cell measurements and/or spectral cross-talk in the microscope used.[15] Despite the observed reduction of ΔR_{max} in live cell experiments, the dynamic range of our MTX-uSnifit compares favorably to other FRET-based protein sensors.[2,3] Next, we investigated the dynamics of sensor opening and closing on HEK293T cells. The kinetics of sensor opening on labeled cells (BG3 + Tet2) in the presence of 0.5 mM MTX were fitted to a single exponential function, yielding a $t_{1/2,open}$ which is defined as the time to open half of the sensor population, of 17.3 ± 1.8 s (Figure S8a). This value is similar to the value we measured *in vitro* ($t_{1/2,open}^{in\ vitro}$ = 22.3 ± 2.4 s, Figure S9). After washing out MTX, we observed a $t_{1/2,close}$ of 116.1 ± 6.3 s (Figure S8b). It should be noted that the kinetics of sensor opening and closing are mainly governed by the dissociation rate constant (k_{off}) of bound tethered ligand and analyte, respectively.[4b] The 5-fold larger value of $t_{1/2,close}$ relative to $t_{1/2,open}$ can thus be explained by the smaller k_{off} of MTX relative to TMP.[16] Finally, we measured K_d^{comp} for MTX on a single cell by perfusion with different concentrations of MTX (Figures 5d,e

DOI: 10.1021/jacs.6b03034
J. Am. Chem. Soc. 2016, 138, 5258−5261

and S10). The K_d^{comp} was found to be 9.1 ± 2.2 μM, which is comparable to the value measured *in vitro* (Table 1). Overall, our live-cell imaging experiments demonstrate that (i) specific dual labeling of proteins using unnatural amino acid technology and SNAP-tag on the surfaces of live cells is possible and (ii) functional uSnifits with large dynamic ranges can be semi-synthesized on live cells.

In summary, by combining the Snifit principle with unnatural amino acid technology, we introduce a simple and generally applicable method to generate ratiometric biosensors with unprecedented dynamic range. We furthermore demonstrate that such sensors can be semisynthesized on the surfaces of live cells. The performance of these uSnifits is such that they should find applications both in basic research and diagnostics.

■ ASSOCIATED CONTENT

Supporting Information

The Supporting Information is available free of charge on the ACS Publications website at DOI: 10.1021/jacs.6b03034.

Experimental details and data (PDF)

■ AUTHOR INFORMATION

Corresponding Author

*kai.johnsson@epfl.ch

Notes

The authors declare no competing financial interest.

■ ACKNOWLEDGMENTS

This work was supported by funding from the Swiss National Science Foundation, the Lithuanian-Swiss cooperation program (no. CH-3-ŠMM-01/11), the NCCR Chemical Biology, and EPFL. We thank Dr. Lemke E. A. for the pEvol plasmids and Griss R, Schena A, Farrants H, Broichhagen J, Reymond L, and Hovius R for corrections of the manuscript.

■ REFERENCES

(1) (a) Dunn, K. W.; Mayor, S.; Myers, J. N.; Maxfield, F. R. *FASEB J.* **1994**, *8*, 573. (b) Mank, M.; Griesbeck, O. *Chem. Rev.* **2008**, *108*, 1550.

(2) (a) Newman, R. H.; Fosbrink, M. D.; Zhang, J. *Chem. Rev.* **2011**, *111*, 3614. (b) Lalonde, S.; Ehrhardt, D. W.; Frommer, W. B. *Curr. Opin. Plant Biol.* **2005**, *8*, 574.

(3) (a) Pérez Koldenkova, V.; Nagai, T. *Biochim. Biophys. Acta, Mol. Cell Res.* **2013**, *1833*, 1787. (b) Hessels, A. M.; Merkx, M. *Metallomics* **2015**, *7*, 258. (c) Liang, R.; Broussard, G. J.; Tian, L. *ACS Chem. Neurosci.* **2015**, *6*, 84. (d) Zhao, Y.; Yang, Y. *Curr. Opin. Biotechnol.* **2015**, *31*, 86. (e) Arosio, D.; Ratto, G. M. *Front. Cell. Neurosci.* **2014**, *8*, 258.

(4) (a) Brun, M. A.; Tan, K. T.; Nakata, E.; Hinner, M. J.; Johnsson, K. *J. Am. Chem. Soc.* **2009**, *131*, 5873. (b) Brun, M. A.; Griss, R.; Reymond, L.; Tan, K.-T.; Piguet, J.; Peters, R. J. R. W.; Vogel, H.; Johnsson, K. *J. Am. Chem. Soc.* **2011**, *133*, 16235.

(5) Keppler, A.; Gendreizig, S.; Gronemeyer, T.; Pick, H.; Vogel, H.; Johnsson, K. *Nat. Biotechnol.* **2003**, *21*, 86.

(6) Gautier, A.; Juillerat, A.; Heinis, C.; Corrêa, I. R.; Kindermann, M.; Beaufils, F.; Johnsson, K. *Chem. Biol.* **2008**, *15*, 128.

(7) (a) Masharina, A.; Reymond, L.; Maurel, D.; Umezawa, K.; Johnsson, K. *J. Am. Chem. Soc.* **2012**, *134*, 19026. (b) Brun, M. A.; Tan, K.-T.; Griss, R.; Kielkowska, A.; Reymond, L.; Johnsson, K. *J. Am. Chem. Soc.* **2012**, *134*, 7676. (c) Schena, A.; Johnsson, K. *Angew. Chem., Int. Ed.* **2014**, *53*, 1302.

(8) (a) Wang, L.; Schultz, P. G. *Angew. Chem., Int. Ed.* **2005**, *44*, 34. (b) Lang, K.; Chin, J. W. *Chem. Rev.* **2014**, *114*, 4764.

(9) (a) Haruki, H.; Gonzalez, M. R.; Johnsson, K. *PLoS One* **2012**, *7*, e37598. (b) Liu, W.; Li, F.; Chen, X.; Hou, J.; Yi, L.; Wu, Y. W. *J. Am. Chem. Soc.* **2014**, *136*, 4468. (c) Griss, R.; Schena, A.; Reymond, L.; Patiny, L.; Werner, D.; Tinberg, C. E.; Baker, D.; Johnsson, K. *Nat. Chem. Biol.* **2014**, *10*, 598.

(10) (a) Neumann, H.; Peak-Chew, S. Y.; Chin, J. W. *Nat. Chem. Biol.* **2008**, *4*, 232. (b) Mukai, T.; Kobayashi, T.; Hino, N.; Yanagisawa, T.; Sakamoto, K.; Yokoyama, S. *Biochem. Biophys. Res. Commun.* **2008**, *371*, 818. (c) Yanagisawa, T.; Ishii, R.; Fukunaga, R.; Kobayashi, T.; Sakamoto, K.; Yokoyama, S. *Chem. Biol.* **2008**, *15*, 1187. (d) Nguyen, D. P.; Lusic, H.; Neumann, H.; Kapadnis, P. B.; Deiters, A.; Chin, J. W. *J. Am. Chem. Soc.* **2009**, *131*, 8720. (e) Fekner, T.; Li, X.; Lee, M. M.; Chan, M. K. *Angew. Chem., Int. Ed.* **2009**, *48*, 1633. (f) Plass, T.; Milles, S.; Koehler, C.; Schultz, C.; Lemke, E. A. *Angew. Chem., Int. Ed.* **2011**, *50*, 3878. (g) Lang, K.; Davis, L.; Wallace, S.; Mahesh, M.; Cox, D. J.; Blackman, M. L.; Fox, J. M.; Chin, J. W. *J. Am. Chem. Soc.* **2012**, *134*, 10317. (h) Lang, K.; Davis, L.; Torres-Kolbus, J.; Chou, C.; Deiters, A.; Chin, J. W. *Nat. Chem.* **2012**, *4*, 298.

(11) (a) Plass, T.; Milles, S.; Koehler, C.; Szymański, J.; Mueller, R.; Wießler, M.; Schultz, C.; Lemke, E. A. *Angew. Chem., Int. Ed.* **2012**, *51*, 4166. (b) Nikić, I.; Plass, T.; Schraidt, O.; Szymański, J.; Briggs, J. A. G.; Schultz, C.; Lemke, E. A. *Angew. Chem., Int. Ed.* **2014**, *53*, 2245.

(12) Adams, J.; Johnson, K.; Matthews, R.; Benkovic, S. J. *Biochemistry* **1989**, *28*, 6611.

(13) Vogel, S. S.; Van der Meer, B. W.; Blank, P. S. *Methods* **2014**, *66*, 131.

(14) (a) Bojkowska, K.; Santoni de Sio, F.; Barde, I.; Offner, S.; Verp, S.; Heinis, C.; Johnsson, K.; Trono, D. *Chem. Biol.* **2011**, *18*, 805. (b) Chin, J. W. *Annu. Rev. Biochem.* **2014**, *83*, 379.

(15) (a) Broussard, J. A.; Rappaz, B.; Webb, D. J.; Brown, C. M. *Nat. Protoc.* **2013**, *8*, 265. (b) Geddes, C. D.; Lakowicz, J. R. *Reviews in Fluorescence 2007*; Springer: New York, 2009; Vol. 4, pp 87−101.

(16) Carroll, M. J.; Mauldin, R. V.; Gromova, A. V.; Singleton, S. F.; Collins, E. J.; Lee, A. L. *Nat. Chem. Biol.* **2012**, *8*, 246.

DOI: 10.1021/jacs.6b03034
J. Am. Chem. Soc. 2016, 138, 5258−5261